PASJ: Publ. Astron. Soc. Japan **48**, 671–677 (1996)

Uniformity in the Temperature and Metallicity of the X-Ray Emitting Gas in the Abell 1060 Cluster of Galaxies

Takayuki TAMURA,[1] Charles S. DAY,[2] Yasushi FUKAZAWA,[1] Isamu HATSUKADE,[3]
Yasushi IKEBE,[4] Kazuo MAKISHIMA,[1] Richard F. MUSHOTZKY,[2]
Takaya OHASHI,[5] Kazuhiro TAKENAKA,[3] and Koujun YAMASHITA [6]

[1] *Department of Physics, School of Science, The University of Tokyo, Hongo, Bunkyo-ku, Tokyo 113*
[2] *Code 666, NASA Goddard Space Flight Center, Greenbelt, MD 20771, U.S.A.*
[3] *Faculty of Engineering, Miyazaki University, Gakuen-Kibanadai-Nishi, Miyazaki 889-21*
[4] *Cosmic Radiation Laboratory, The Institute for Physical and Chemical Research, Wako, Saitama 351-01*
[5] *Department of Physics, Tokyo Metropolitan University, Minami-Ohsawa, Hachioji, Tokyo 192-03*
[6] *Department of Astrophysics, School of Science, Nagoya University, Furo-cho, Chikusa-ku, Nagoya 464-01*

(Received 1995 November 6; accepted 1996 July 24)

Abstract

The results from ASCA observations of the Abell 1060 cluster of galaxies are presented. Spatially sorted X-ray spectra were used to derive the distributions of the temperature and metallicity in the X-ray emitting gas of the cluster. Within $\sim 20'$ (or 400 kpc assuming $H_0 = 50$ km s^{-1} Mpc^{-1}) of the cluster center, the gas temperature has been found to be radially constant at $3.1^{+0.3}_{-0.5}$ keV (or 3.1 ± 0.2 keV within $\sim 10'$), and the 2–10 keV luminosity was estimated to be 2×10^{43} erg s^{-1} . An upper limit on the cool emission component at the cluster center was derived to be 6×10^{41} erg s^{-1} in 0.5–3 keV, assuming that it has a temperature of 1 keV. Although the metallicity is consistent with being radially constant at 0.3 relative to solar value, the present observations do not constrain the abundance well beyond $10'$, allowing values in the range from 0.2 to 0.4 solar value. There is some indication that O, Ne, and Si are more abundant than Fe and Ni, when compared to the solar-abundance ratios. These results suggest the importance of galactic winds driven by type-II supernovae during the early phase of galaxy formation. In comparison with the Centaurus and Virgo clusters, discussions are made concerning the possible role of the cD galaxy in generating a metal concentration and a cool X-ray component at the cluster center.

Key words: Galaxies: abundances — Galaxies: clustering — Galaxies: clusters: individual: (Abell 1060) — X-rays: galaxies

1. Introduction

Clusters of galaxies are filled with an X-ray emitting intracluster medium (ICM) of temperature 1–10 keV (e.g., Sarazin 1988). Soft X-ray imaging observations with Einstein Observatory (e.g., Jones, Forman 1984) have shown that the observed X-ray surface-brightness profiles are consistent with the hydrostatic isothermal ICM model in most clusters, except in the central regions of some clusters with cD galaxies. The isothermality (except in the central regions) has generally been confirmed in subsequent X-ray observations, with ROSAT in particular.

The metallicity of the ICM provides key information concerning the dynamical and chemical evolution of clusters. Measurements with non-imaging instruments (e.g., Mushotzky 1984; Okumura et al. 1988; Edge, Stewart 1991; Hatsukade 1989; Yamashita 1992) have shown that the ICM has an iron abundance of 0.2–0.4 solar value. Furthermore, Ginga observations of the Virgo cluster by Koyama et al. (1991) have revealed a strong iron concentration around its cD galaxy, M87. The recent ROSAT observations have revealed metallicity distributions in some groups of galaxies and poor clusters. For example, David et al. (1994) found that the iron abundance in the NGC 5044 group is relatively uniform throughout the ICM. However, in other clusters, the ICM metallicity gradient has remained unknown, or controversial, as in the case of the Perseus cluster (Mushotzky et al. 1981; Ponman et al. 1990; Arnaud et al. 1993; Kowalski et al. 1993).

Accurate measurements of the spatial distributions of the major elements have been enabled for the first time by ASCA (Tanaka et al. 1994). Early ASCA observations show that the iron abundance is relatively uniform in a fair number of clusters (Ohashi et al. 1994), ex-

cept in rich clusters with substructures (Briel et al. 1991; Markevitch et al. 1994; Arnaud et al. 1994). However, in the Centaurus cluster, Fukazawa et al. (1994) have discovered a strong metal concentration around its cD galaxy, NGC 4696, where a cool emission component with a temperature of $kT \sim 1$ keV is also seen (Fabian et al. 1994). This is reminiscent of the Virgo cluster (Koyama et al. 1991; Matsumoto et al. 1994).

In order to further investigate the issue of spatial variations of the ICM properties, we analyze here the ASCA data of the poor cluster Abell 1060 (A1060 for short). At a redshift of $z = 0.0114$, A1060 is one of the nearest members in the Abell clusters, and has a relatively low temperature ($\sim$ 3 keV) according to previous observations (Mitchell, Mushotzky 1980; Singh et al. 1988; Hatsukade 1989; David et al. 1993). In addition, only a relatively low level of cooling flow has been quoted for A1060 (Stewart et al. 1984; Singh et al. 1988) among poor clusters. These properties make A1060 ideal for spatially resolved spectroscopy.

Our results show that the ICM temperature and metallicity are spatially both quite uniform in A1060, in contrast to the case of the Centaurus and Virgo clusters. We discuss possible causes for these differences. We assume $H_0 = 50$ km s^{-1} Mpc^{-1} throughout.

2. Observations

ASCA observations of A1060 were performed on 1993 June 28 and 29 during the performance-verification (PV) phase. We obtained a net exposure time of $\sim$ 30 ks with the GIS (Gas Imaging Spectrometer; Ohashi et al. 1996) in the PH normal mode and the SIS (Solid-state Imaging Spectrometer; Burke et al. 1991) in the 4-CCD bright mode. Some spectroscopic results from these observations have already been reported by Mushotzky et al. (1996; hereafter MLA96), together with those of three other clusters. In this paper we report on more detailed results concerning A1060.

Figure 1 shows an X-ray image of A1060 in 0.6–8.0 keV obtained with the GIS. The X-ray emission is thus distributed fairly symmetrically, with the brightness centroid coincident with a pair of massive elliptical galaxies, NGC 3311 and NGC 3309. Note that NGC 3311 is classified as a cD galaxy, while NGC 3309 is a giant elliptical (Västerberg et al. 1991).

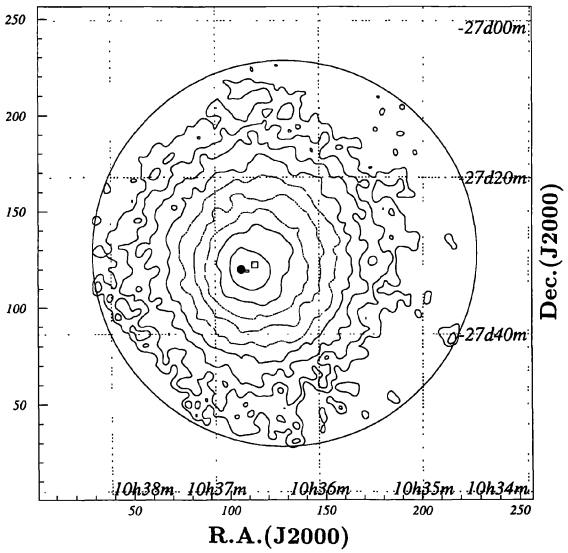

Fig. 1. X-ray image of the Abell 1060 taken with the GIS in 0.6–8 keV. This is smoothed with a Gaussian filter with $\sigma = 0.'5$, but not corrected for the XRT vignetting or partial shadows due to the detector support ribs. The contour levels are logarithmically spaced. The sky coordinates are J2000, in which NGC 3311 (marked •) and NGC 3309 (marked □) are located at ($10^h34^m43^s, -27°31'41''$) and ($10^h36^m36^s, -27°31'6''$), respectively. The circle roughly corresponds to the GIS FOV.

3. Data Analysis and Results

3.1. Average Spectra

For spectroscopy, we have screened events from each detector using the standard data-selection criteria; i.e., geomagnetic cutoff rigidity > 6 and > 8 GeV c^{-1} for the SIS and GIS, respectively, earth elevation angle $> 10°$ for the GIS, while $> 10°$ (dark earth) and $> 25°$ (sunlit earth) for the SIS. The GIS events were then summed over the two detectors (GIS-S2 and GIS-S3), and the SIS events were summed over CCD chips after appropriate gain corrections, but separately for the two detectors, SIS-S0 and SIS-S1. Figure 2 shows the GIS spectra of A1060 thus accumulated over three concentric regions with different projected radii ($r < 3'$, $r = 3'$–$10'$, and $r = 10'$–$20'$) from the emission centroid, while figure 3 shows the SIS spectra accumulated for two concentric regions ($< 3'$ and $3'$–$10'$). Note that the GIS has a circular field of view (FOV) of $\sim 45'$ diameter, while the SIS (in 4-CCD mode) has a $22' \times 22'$ rectangular FOV. Each spectrum is presented after subtracting the corresponding background spectrum, which was made by extracting events over the identical region on the same detector using the data from blank-sky pointings. No significant difference can be seen among the three GIS spectra, nor between the two SIS spectra.

In order to study the spatially averaged properties of the emission, we jointly fitted the GIS and SIS spectra within $10'$ of the cluster center, with an isothermal Raymond-Smith (1977) plasma emission model modified by the photoelectric absorption. (In practice, the S0, S1,

Table 1. Results of the single-temperature Raymond-Smith model fits.*

	Inner region ($r < 10'$)		Outer region ($10' < r < 20'$)
Detector	GIS + SIS		GIS
Abundance ratio	Solar ratios	Variable ratios‡	Solar ratios
kT (keV)	3.11 (3.05–3.15)	3.10 (3.06–3.17)	3.03 (2.92–3.15)
N_H (10^{20}cm^{-2})	7.6 (7.3–8.5)	8.3 (7.7–8.8)	6.00 (fixed)
Metallicity†	0.31 (0.29–0.34)	...	0.30 (0.21–0.39)
O, Ne, Si	...	0.43 (0.35–0.54)	...
Mg	...	0.16 (< 0.40)	...
S	...	0.25 (0.14–0.35)	...
Ar, Ca	...	0.0 (< 0.09)	...
Fe, Ni	...	0.31 (0.29–0.34)	...
χ^2/ν	1058/882	1032/878	193.9/176

* The error regions in parentheses refer to single-parameter 90% confidence limits.
† Overall metallicity in solar unit, mainly determined by the Fe-K line.
‡ Abundances of He, C, and N relative to H are assumed to be 1.0, 0.5, and 0.5 times the solar ratios.

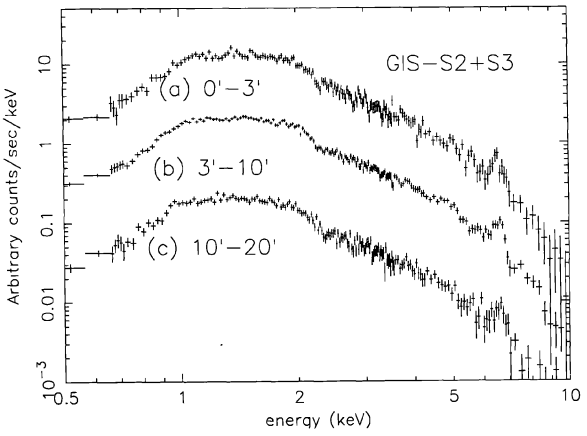

Fig. 2. GIS spectra (sum of the two sensors) of A1060 for three regions: (a) $r < 3'$, (b) $3' < r < 10'$, and (c) $10' < r < 20'$, where r is the projected radius from the emission centroid. The background spectra of the blank sky were subtracted. For clarity, the spectra are vertically offset from one another.

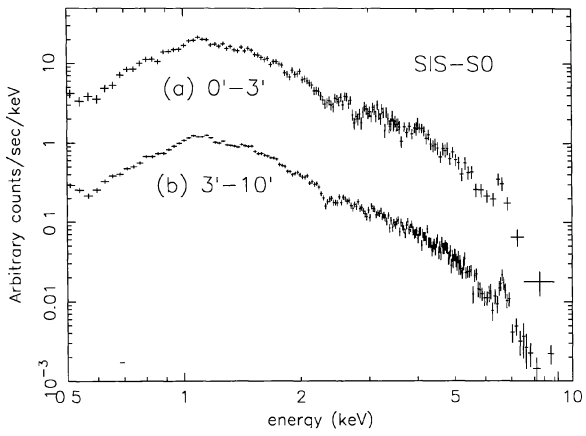

Fig. 3. SIS-S0 spectra (sum of all chips) for two regions: (a) $r < 3'$, and (b) $3' < r < 10'$. The background spectra of the blank sky were subtracted. The SIS-S1 spectra (not shown) are similar.

and S2 + S3 spectra were fitted simultaneously with the common model spectrum.) The abundance ratios among elements heavier than helium were fixed to be solar, and the solar Fe/H ratio was taken to be 4.68×10^{-5} by number. As shown in table 1 (left column), the fit is roughly acceptable, yielding a temperature of $\sim$ 3.1 keV and a metal abundance of $\sim$ 0.3-times solar (which is mostly determined by the iron K-line). Here, and hereafter, all of the errors and limits refer to single-parameter 90% confidence levels. The derived neutral column density of $N_H = 7.6 \times 10^{20}$ cm^{-2} is similar to the galactic value of 6×10^{20} cm^{-2} .

To evaluate the spectrum falling outside the SIS FOV, we fitted the GIS spectrum for a ring-shaped region with projected radii of 10′–20′ using the same isothermal model. The fit is acceptable, and the obtained best-fit parameters (table 1; right column) agree with those for < 10′ derived with the SIS and GIS. Furthermore, the temperature of 3.4 ± 0.5 keV, derived by Singh et al. (1988) using the EXOSAT ME having a 45′ FWHM field of view, is consistent with our results. We therefore suggest that the ICM properties of A1060 are spatially rela-

tively uniform. The 2–10 keV X-ray luminosity becomes $\sim 2\times10^{43}$ erg s^{-1} within 20′, or $\sim$ 400 kpc, in agreement with the past results (e.g., Jones, Forman 1984). The Einstein MPC measurement indicated a slightly higher temperature (3.6–4.3 keV; David et al. 1993). Furthermore, the ASCA results are inconsistent with the two-temperature nature of the A1060 emission observed with Ginga ($kT \sim 2.6$ keV and ~ 7.4 keV; Hatsukade 1989) as well as HEAO-1 (Mitchell, Mushotzky 1980). We suggest that the larger fields of view of the Ginga LAC and the HEAO-A2 were contaminated by a hard background source. When we ignore the hotter component in the Ginga spectrum and assume the continuum temperature to be 3.1 keV, the iron abundance of 0.40 ± 0.03 solar, quoted by Hatsukade (1989), translates to 0.36 ± 0.07, in agreement with the present measurements.

3.2. *Temperature and Metallicity Gradients*

To further investigate the spatial variations of the ICM properties, we next derived the spectra in finer annuli around the X-ray centroid, and fit each with the same model. Within 10′ we jointly used the SIS-S0, SIS-S1, and GIS-(S2 + S3) data, while outside 10′ we used only the GIS data.

The fit has been successful for all annuli, with the reduced chi-squared in the range 1.02–1.18 and 0.98–1.08 for a typical degree of freedom of 527 and 322 for the joint SIS/GIS fits and the GIS fits, respectively. The thus obtained best-fit parameters and the 90% confidence errors are shown in figure 4 as a function of the projected radius from the cluster center. Thus, as measured in eight annuli within $\sim$ 20′ around the cluster center, the radial distributions of the temperature and metallicity are both consistent with being constant. The temperature lies in the range $3.1^{+0.3}_{-0.5}$ keV, and is better constrained to be 3.1 ± 0.2 keV within $\sim$ 10′. The metallicity within $\sim$ 10′ of the cluster center falls in the range 0.3 ± 0.1 solar value, although it is not well constrained beyond $\sim$ 10′. The column density of the absorbing matter is also constant, with an almost insignificant excess above the galactic value. These results confirm our inference made in the previous subsection that the ICM in A1060 has spatially uniform properties.

3.3. *Limits on the Central Cool Emission*

Through a deprojection analysis of the X-ray surface brightness profiles obtained with the Einstein IPC (Stewart et al. 1984) and the EXOSAT LE (Singh et al. 1988), a weak cooling flow was indicated in the core region of A1060 with a mass deposition rate $\dot{M}$ of $\sim 10\ M_\odot$ yr^{-1}. An approximate formula relates $\dot{M}$ to the bolometric excess luminosity L_c associated with the cooling flow as $L_c = \dfrac{5\dot{M}kT_c}{2\mu m_p}$ (e.g., Fabian et al. 1991),

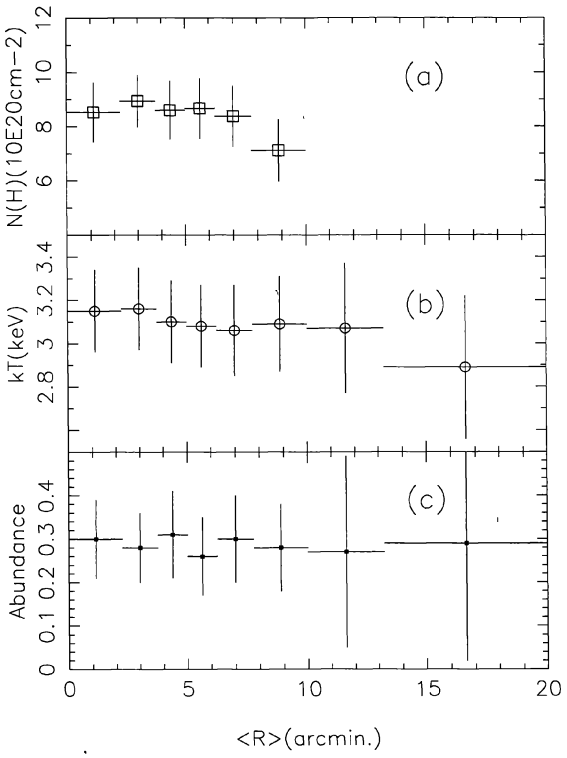

Fig. 4. Best-fit parameters vs. projected radius derived from spectral fits. (a) Column density, (b) gas temperature, and (c) metal abundance in solar units ; the vertical error bars show the 90% confidence limits. For $r < 10'$, the GIS and SIS data are jointly used. For $r > 10'$, only the GIS data were used, and the column density was fixed to the galactic value.

where kT_c is the temperature at the edge of the cooling region, m_p is the proton mass, and $\mu \sim 0.6$ is the mean molecular weight. Assuming $kT_c = 3.1$ keV, as observed, we obtain a prediction of $L_c \sim 8\times10^{42}$ erg s^{-1} for A1060, which is in fact quite large.

In a search for the predicted cool emission, we added another Raymond-Smith component to fit the innermost ($r < 3'$) SIS and GIS spectra. We allowed the hotter Raymond-Smith component to be absorbed by a column, N_H, while the cooler Raymond-Smith component to be absorbed by $N_H + N'_H$, where $N'_H \geq 0$ represents possible internal excess absorption (White et al. 1991). The metal abundances of both components were assumed to be the same, while the two temperatures as well as N_H and N'_H were left free. However, the fit was not improved by introducing the cooler component (χ^2/ν changed from 610/519 to 609/516), as compared to the single temperature fit ($kT = 3.17$ keV, $N_H = 8.2$ cm^{-2} , metallicity $= 0.29$), implying that the ASCA spectra do not require an additional cool component.

To set an upper limit on the cool emission, we then fixed the cooler temperature to be 1.0 keV and the metallicity to be 0.3 solar. We also fixed $N_{\rm H}$ at the galactic value, and $N'_{\rm H}$ at 1×10^{21} cm^{-2}, which is typically found in cooling flows (White et al. 1991). The thus obtained 90% upper limit on the 0.5–3 keV cool-component flux is 5×10^{-13} erg s^{-1} cm^{-2}, while the hotter temperature turned out to be 3.2 keV. If there is no excess absorption ($N'_{\rm H} = 0$), the upper limit would be 4×10^{-13} erg s^{-1} cm^{-2}, and if the metallicity of the cooler component is higher than the global value, the upper limit would become small (e.g., the upper limit of 3×10^{-13} erg s^{-1} cm^{-2} for the metallicity of 1 solar value). The nominal upper-limit flux yields a 0.5–3.0 keV upper-limit luminosity of $\sim 6 \times 10^{41}$erg s^{-1}, after correcting for the event spill-over outside the 3′ integration radius. This luminosity is $\sim 3\%$ of the total luminosity in the same band and by an order of magnitude lower than the expected $L_{\rm c}$, although the discrepancy may be relaxed by taking into acount the more complex temperature distribution in a cooling flow.

3.4. Abundance Ratios

The uniformity of the ICM properties in A1060, together with the relatively low temperature, provides an excellent opportunity to determine the relative metal abundances, and hence, the relative importance of type-I and type-II supernovae (MLA96), since around this temperature we expect to (and actually we do) see K-emission lines from various elements from O through Fe (MLA96).

For a quantitative evaluation of the abundance ratios, we return to the SIS and GIS spectra from $r < 10'$, and fit them simultaneously using a variable-abundance Raymond-Smith model. The major elements were grouped into five in the fitting, and a common (but free) abundance was assigned to each group. The five groups are: (1) O, Ne, and Si, (2) Mg, (3) S, (4) Ar and Ca, and (5) Fe and Ni. The reason to single out Mg is to avoid a false coupling between the Mg-K and Fe-L lines, as pointed out by Fabian et al. (1994).

We show the results of this variable abundance fit in table 1 (middle column). The obtained O-Ne-Si abundance is marginally larger than the Fe-Ni abundance. The S abundance seems to be similar to the Fe abundance, or somewhat lower, while the Ar-Ca abundance is rather low. The Mg abundance should be neglected (Fabian et al. 1994). The fit is no longer improved by further allowing the O, Ne, and Si abundances to vary independently (their best-fit abundances become similar with one another within relatively large uncertainties). In our analysis we used the same ASCA data sets as used for MLA96. Our analysis differed in that they excluded the central 3′ region, which we did not, and they primarily used SIS data, while we jointly used the SIS/GIS data. Our results are thus consistent with theirs.

4. Discussion

4.1. Origin of Heavy Elements

Through spatially sorted spectroscopy incorporating eight annular spectra, we have found that the ICM in A1060 has rather uniform properties from the center out to $\sim$ 200 kpc, and possibly to $\sim$ 400 kpc. Therefore, the ICM in this cluster is supposed to be well virialized, and the metal-rich gas ejected from individual member galaxies may be thoroughly mixed into ICM via, e.g., ram-pressure stripping.

The present studies and those of MLA96 suggest that O, Ne, and Si are overabundant relative to Fe in A1060 (and in some other clusters; MLA96). This supports the earlier suggestion that frequent type-II supernovae (SNe), presumably during the burst-like star formation stage early in the cluster evolution, were the dominant origin of the heavy elements in the ICM (Arimoto, Yoshii 1987; White et al. 1991; David et al. 1991). Therefore, in addition to the ram-pressure stripping, a strong galactic wind driven by a series of type-II SN explosions may have efficiently transported the metals away from the vicinity of individual galaxies. Such a scenario is at least in qualitative agreement with the surprisingly low metallicities in the hot gas of non-cD elliptical galaxies, as observed with BBXRT (Serlemitsos et al. 1993), ROSAT (Forman et al. 1993), and ASCA (Awaki et al. 1994; Loewenstein et al. 1994; Matsushita et al. 1994). However, quantitative models of metal transport are obviously yet to be constructed.

The ICM is generally thought to exhibit a more extended mass distribution than the stellar component, which would predict a gradual abundance decrease outwards. It is yet to be examined whether the present results from A1060 are consistent with this simple view.

4.2. Comparison with the Virgo and Centaurus Clusters

As argued by Ohashi et al. (1994) based on early ASCA results, the abundance gradient in the cluster ICM is a complicated issue. Some rich clusters show non-radial variations in the temperature and/or abundance (Briel et al. 1991; Arnaud et al. 1994; Markevich et al. 1994). Even putting these examples aside, the present results on A1060 make an outstanding contrast to the two poor-cD clusters with comparable luminosities: the Virgo cluster and the Centaurus cluster. In fact, Virgo (Koyama et al. 1991; Matsumoto et al. 1994) and Centaurus clusters (Fukazawa et al. 1994; Ikebe 1995) both exhibit a factor of 3–5 metallicity increase at the center, as well as a strong cool emission with $kT \sim 1$ keV, whose luminosity amounts to 10–20% of the total luminosity.

A comparison among these ASCA results on poor clusters suggests a close correlation between the metal concentration and the central cool emission (Ohashi et al. 1994). Virgo and Centaurus clusters can be considered to be on one extreme of this correlation, clearly exhibiting both phenomena. On the contrary, A1060, showing neither phenomenon, can be regarded as the other extreme. The Fornax cluster, with a rather uniform temperature and metallicity, is similar to A1060 in this respect. An intermediate case may be AWM 7, which exhibits a mild (factor $\sim$ 1.5) metal concentration and some evidence of a central temperature drop (Ohashi et al. 1994; Xu et al. 1996). Furthermore, the two phenomena appear to be closely related to the presence of a cD galaxy, because they take place over a typical region (50–100 kpc in radius) governed by the cD galaxy. Above all, the abundance concentration would be difficult to explain without invoking the metal-rich gas produced by the cD galaxy, even though the temperature drop could be explained in terms of the cooling flow. Then, what makes the difference between the A1060/Fornax type objects and the Virgo/Centaurus type ones?

We notice that the cD galaxy of A1060, NGC 3311, is optically $\sim$ 3-times fainter than more typical cD galaxies, e.g., M87 in the Virgo cluster and NGC 4696 in the Centaurus cluster. Furthermore, NGC 3311 is apparently interacting with the giant elliptical companion NGC 3309 at a projected separation of only 35 kpc. Their relative motion is expected to disturb the cooling flow by agitating the ICM. Also, this makes NGC 3311 subject to ram-pressure stripping, like in the case of ordinary non-cD galaxies. Then, the metal-rich interstellar medium (ISM) of NGC 3311, which is intrinsically less substantial, will be continuously stripped by the ICM, leaving little trace of the metal concentration. A similar case may be the Fornax cluster, in which the cD galaxy NGC 1399 has a close companion, NGC 1404, and is offset from the cluster center (Makishima 1995b; Ikebe et al. 1995). Indeed, the emission from Fornax/NGC 1399 is isothermal at 1.2 keV, except for the central 30 kpc (Rangarajan et al. 1995), with an insignificant metallicity concentration.

In contrast, M87 and NGC 4696 are very massive, and likely to be sitting still at the bottom of the cluster potential. Thus, the ram-pressure stripping will not work, and much of their ISM will remain trapped in the local galaxy potential, which has a virial temperature of $\sim$ 1 keV. To insulate the ISM against heat conduction from ICM (Takahara, Takahara 1979), and to suppress the radiative cooling instability, magnetic fileds may be needed (Rosner, Tucker 1989; Makishima 1994, 1995a, 1995b). Since the ISM must be metal enriched by the type-Ia SNe in the cD galaxy over the Hubble time, we thus expect a metal concentration and cool emission to occur within the cD potential. Actually, Fukazawa et al. (1994) have shown that the iron in the metal-enriched portion of the Centaurus ICM can be supplied by the cD galaxy over the Hubble time. Thus, the differences in the efficiency of the ISM confinement may discriminate "genuine" cD galaxies against interacting cD's and non-cD ellipticals.

5. Conclusion and Future Prospect

The present ASCA results concerning A1060 can be summarized by the following three points:

1. The metallicity of the ICM in A1060 is consistent with being radially uniform at $\sim$ 0.3 times the solar value up to $\sim$ 400 kpc from the cluster center.
2. The emission is consistent with being isothermal at $kT \sim 3.1$ keV.
3. The 0.5–3 keV luminosity of cool emission in the central region is at most $\sim$ 3% of the total luminosity of the cluster in the same band.

The first result, along with our derived abundance ratios, points to the possibility that the heavy elements in the ICM were produced mainly by type-II SNe in member galaxies, and transported to the intra-cluster space via ram-pressure stripping and the galactic wind. However, the relatively low Ar and Ca abundances are somewhat puzzling, since these must be produced by type-II SNe. From the latter two results, we infer that the $kT = 3.1$ keV ICM almost completely fills the local potential well of the cD galaxy NGC 3311. Such a condition may be realized if the cD galaxy is to some extent subject to ram-pressure stripping, because the metal-rich cool gas ejected from the cD galaxy will be swept away, just like in ordinary cluster member galaxies. If instead the gas ejected from the cD galaxy mostly remains trapped within the cD potential, we expect a cool emission and abundance increase to take place at the center. We associate such a condition to the Centaurus and Virgo clusters of galaxies.

Finally, these considerations lead us to speculate that the heavy elements in the cluster ICM are made up of two separate components. One has a uniform spatial distribution and an enhanced Si/Fe ratio, presumably ejected by many member galaxies during the early wind phase. The other component, which is not always seen, is confined to the vicinity of the cD galaxy, and has a more solar-type abundance ratios, presumably contributed mainly by the type-Ia SNe and stellar mass loss of the cD galaxy. A further study of the abundance ratios in the metal-enriched regions of the Virgo/Centaurus type clusters will be of great importance.

The authors wish to express their thanks to A.C. Fabian for helpful comments on this paper.

References

Arimoto N., Yoshii Y. 1987, A&A 173, 23

Arnaud K.A., Mushotzky R., Ezawa H., Fukazawa Y., Ohashi T., Bautz M., Crewe G., Gendreau K. et al. 1994, ApJ 436, L67

Arnaud K.A., Mushotzky R., Serlemitsos P., Boldt E., Holt S., Jahoda K., Marshall F., Petre R. et al. 1993, in Proc. Ginga Memorial Symposium, ed F. Makino, F. Nagase (ISAS, Sagamihara) p114

Awaki H., Mushotzky R., Tsuru T., Fabian A.C., Fukazawa Y., Loewenstein M., Makishima K., Mihara T. et al. 1994, PASJ 46, L65

Briel U.G., Henry J.P., Schwarz R.A., Boehringer H., Ebeling H. 1991, A&A 246, L10

Burke B.E., Mountain R.W., Harrison D.C., Bautz M.W., Doty J.P., Ricker G.R., Daniels P.J. 1991, IEEE Trans. ED-38, 1069

David L.P., Forman W., Jones C. 1991, ApJ 380, 39

David L.P., Jones C., Forman W. 1994, ApJ 428, 544

David L.P., Slyz A., Jones C., Forman W., Vrtilek D., Arnaud K. 1993, ApJ 412, 479

Edge A.C., Stewart G.G. 1991, MNRAS 252, 414

Fabian A.C., Arnaud K.A., Bautz M.W., Tawara Y. 1994, ApJ 436, L63

Fabian A.C., Nulsen P.E.J., Canizares C.R. 1991, A&AR 2, 191

Forman W., Jones C., David L., Franx M., Makishima K., Ohashi T. 1993, ApJ 418, L55

Fukazawa Y., Ohashi T., Fabian A.C., Canizares C.R., Ikebe Y., Makishima K., Mushotzky R.F., Yamashita K. 1994, PASJ 46, L55

Hatsukade I. 1989, PhD thesis, Osaka University

Ikebe Y. 1995, PhD thesis, The University of Tokyo

Ikebe Y., Ezawa H., Fukazawa Y., Hirayama M., Ishisaki Y., Kikuchi K., Kubo H., Makishima K. et al. 1996, Nature 379, 472

Jones C., Forman W. 1984, ApJ 276, 38

Kowalski M.P., Cruddace R.G., Snyder W.A., Fritz G.G., Ulmer M.P., Fenimore E.E. 1993, ApJ 412, 489

Koyama K., Takano S., Tawara Y. 1991, Nature 350, 135

Loewenstein M., Mushotzky R., Tamura T., Ikebe Y., Makishima K., Matsushita K., Awaki H., Serlemitsos P. 1994, ApJ 426, L75

Makishima K. 1994, in New Horizon of X-Ray Astronomy, ed F. Makino, T. Ohashi (Universal Academy Press, Tokyo) p171

Makishima K. 1995a, in Elementary Processes in Dense Plasmas, ed S. Ichimaru, S. Ogata (Addison Wesley, New York) p47

Makishima K. 1995b, in Dark Matter, AIP Proceedings No.336, ed S.S. Holt, C. Bennet, p172

Markevitch M., Yamashita K., Furuzawa A., Tawara Y. 1994, ApJ 436, L71

Matsumoto H., Tsuru T., Awaki H., Koyama K., the ASCA team 1994, in New Horizon of X-Ray Astronomy, ed F. Makino, T. Ohashi (Universal Academy Press, Tokyo) p511

Matsushita K., Makishima K., Awaki H., Canizares C.R., Fabian A.C., Fukazawa Y., Loewenstein M., Matsumoto H. et al. 1994, ApJ 426, L41

Mitchell R., Mushotzky R.F. 1980, ApJ 236, 730

Mushotzky R.F. 1984, Phys. Scrip. T7, 157

Mushotzky R.F., Holt S.S., Smith B.W., Boldt E.A., Serlemitsos P.J. 1981, ApJ 244, L47

Mushotzky R.F., Loewenstein M., Arnaud K.A., Tamura T., Fukazawa Y., Matsushita K., Kikuchi K. 1996, ApJ 466, 686 (MLA96)

Ohashi T., Ebisawa K., Fukazawa Y., Hiyoshi K., Horii M., Ikebe Y., Ikeda H., Inoue H. et al. 1996, PASJ 48, 157

Ohashi T., Fukazawa Y., Ikebe Y., Ezawa H., Tamura T., Makishima K. 1994, in New Horizon of X-Ray Astronomy, ed F. Makino, T. Ohashi (Universal Academy Press, Tokyo) p273

Okumura Y., Tsunemi H., Yamashita K., Matsuoka M., Koyama K., Hayakawa S., Masai K., Hugh J.P. 1988, PASJ 40, 639

Ponman T.J., Bertram D., Church M.J., Eyles C.J., Watt M.P., Skinner G.K., Wilmore A.P. 1990, Nature 347, 450

Rangarajan F.V.N., Fabian A.C., Forman W.F., Jones C. 1995, MNRAS 272, 665

Raymond J.C., Smith B.W. 1977, ApJS 35, 419

Rosner R., Tucker W. 1989, ApJ 338, 761

Sarazin C.L. 1988, X-Ray Emission from Clusters of Galaxies (Cambridge University Press, Cambridge)

Serlemitsos P.J., Loewenstein M., Mushotzky R., Marshall F., Petre R. 1993, ApJ 413, 518

Singh K.P., Westergaard N.J., Schnopper H.W. 1988, ApJ 330, 620

Stewart G.C., Fabian A.C., Jones C., Forman W. 1984, ApJ 285, 1

Takahara M., Takahara F. 1979, Prog. Theor. Phys. 62, 1253

Tanaka Y., Inoue H., Holt S.S. 1994, PASJ 46, L37

Västerberg A.R., Jöräter S., Lindblad P.O. 1991, A&A 247, 335

White D.A., Fabian A.C., Johnston R.M., Mushotzky R.F., Arnaud K.A. 1991, MNRAS 252, 72

White R.E. III 1991, ApJ 367, 69

Xu H., Ezawa H., Fukazawa Y., Kikuchi K., Makishima K., Ohashi T., Tamura T. 1996, PASJ submitted

Yamashita K. 1992, in Frontiers of X-Ray Astronomy, ed Y. Tanaka, K. Koyama (Universal Academy Press, Tokyo) p475